The Effects Of Secondary Doping On Ink-Jet Printed PEDOT:PSS Gas Sensors For VOCs and NO2 Detection

The Effects Of Secondary Doping On Ink-Jet Printed PEDOT:PSS Gas Sensors For VOCs and NO_2 Detection

L. Vigna[1], A. Verna[1], S.L. Marasso[1,2], M. Sangermano[1], P. D'Angelo[2], F.C. Pirri[1,3], M. Cocuzza[1,2]

[1]Dipartimento di Scienza Applicata e Tecnologia (DISAT), Politecnico di Torino, C.so Duca degli Abruzzi 24, 10129 Torino, Italy.

[2]CNR-IMEM, Parco Area delle Scienze, 37a, 43124 Parma, Italy.

[3]Istituto Italiano di Tecnologia, Center for Sustainable Future Technologies, Via Livorno 60, Torino, 10144, Italy.

ABSTRACT: In the study of conductive conjugated polymers, electrical doping has long played an important role. A new polymeric gas sensor has been successfully fabricated by means of an ink-jet printer using a conductive aqueous formulation of poly(3,4-ethylenedioxythiophene) poly(styrene-sulfonate) (PEDOT:PSS). A simple yet robust treatment method for the irreversible secondary doping was performed (by H_2SO_4 and MeOH post-treatments) to enhance conductivity and improve gas sensing performance. The results of FTIR spectroscopy, contact angle and thickness demonstrated the removal of insulating hydrophilic PSS chains and a morphological change leading to a better connection of the hydrophobic conductive PEDOT domains. Real time gas sensing measurements were carried out by exposing the devices with eight different analytes in a low concentrations range of VOCs vapors up to 5% of the saturated vapor pressure, 10 ppm of NO_2 and up to 10% of relative humidity (RH) at 21°C, exploiting dry air as carrier and diluting gas. The gas response, obtained as the ratio between the steady-state resistance variation and the baseline resistance of the device, was evaluated for different PEDOT:PSS post-treated sensors. An unexpected behavior of PEDOT:PSS post-treated with concentrated H_2SO_4 was observed, while MeOH and diluted H_2SO_4 post-treated sensors exhibited improved response towards all investigated analytes. The best performances were obtained towards 5% of ammonia and NO_2 with a gas response of 6% and 28% respectively with the device post-treated with pure methanol and 16% with the sensor post-treated with diluted sulfuric acid. Furthermore, long-term stability and the influence of temperature were evaluated on the fabricated sensors. Altogether, these promising results allow a better understanding of the secondary doping effects on the electrical and sensing properties, paving the way for electronic nose development.

Keywords: PEDOT:PSS, gas sensor, conductive polymer, ink-jet printing, secondary doping, electronic nose

1. INTRODUCTION

Among all intrinsically conductive conjugated polymers, poly(3,4-ethylenedioxythiophene) polystyrene sulfonate (PEDOT:PSS) is a frontrunner material emerging on the scientific scene in the late 1980s and positioning itself as a great candidate for printed electronics [1,2]. It is becoming to organic electronics what silicon is for inorganic electronics [3]. This conjugated polymer appears as

an excellent material due to its peculiar properties like remarkable high electrical conductivity, stability and transparency in the visible range in its doped state associated with a low band gap, easy processability, good mechanical flexibility, low cost and excellent thermal stability [4]. We address the reader to the review article by Groenendaal *et al.* for additional detailed information about the synthesis process, all the properties and characterizations of PEDOT:PSS [5]. The aforementioned properties of PEDOT:PSS has risen its popularity in many research fields and applications that range from: electronics for transparent electrodes capacitors, photodiodes [6,7] and as a hole transport layer of organic LED to antistatic coatings [8]; in sensing and biosensing for the development of Organic Electro Chemical Transistor (OECT) devices [9–14] and the realization of stretchable and 3D printed electronics [15–18]; in neuromorphic systems for the implementation of memristive devices [19]; in additive manufacturing for the exploitation of new conductive composites and 3D printed electronics [20–23]. In this context, thanks to the high potentials of molecular modifications and tunable properties, PEDOT:PSS has been successfully used as chemiresistive gas sensor [16,24–36] especially for Volatile Organic Compounds (VOCs) detection [12,17,37–42] due to the well-known ever growing need to monitor the environmental pollution. Among all the contaminants in air, VOCs such as acetone, ethanol and 2-propanol are the most common and hazardous. Even at very low concentrations these molecules not only contaminate the environment, but also directly affect human's health and climate change [43]. Moreover, nitrogen oxides family (NO_x including NO and NO_2), are notorious pungent toxic oxidizing gases which enter the atmosphere from either natural sources or due to anthropogenic activities [44]. NO_2 emissions are mainly due to fossil fuel combustion, diesel automobile exhaust and biomass burning [45]. Furthermore, they play a central role in the formation of acid rains, photochemical smog and PM 2.5 as well as contributing to the potential greenhouse effect and ozone generation in the atmosphere, but also endanger people's health [46]. Traces of NO_2 can damage the respiratory system and increase the risk of pneumonia and asthma. According to the National Institute for Occupational Safety and Health, when concentration is above 10 ppm, people will start feeling uncomfortable and cause harm to life at concentrations above 20 ppm [47]. Therefore, for all the above reasons, it is urgent to develop high-efficiency gas sensors that can easily detect VOCs and NO_2 at room temperature with high sensitivity, fast response, low detection limit and power consumption.

Organic conductive polymers including polyaniline (PANI), polypyrrole (PPy), polythiophene (PTh) and PEDOT are by far the most studied as gas sensing materials, exploiting their high sensitivity and electrical conductivity, inexpensive synthesis and wide detection range of volatiles [48–50]. PEDOT is itself intrinsically insoluble in all common solvents and very unstable in its neutral state. In order to overcome this problem and facilitate the patterning through printing technologies, PSS was added

to PEDOT in an eco-friendly solvent, i.e. water, making a green sustainable aqueous dispersion in comparison with other toxic organic compounds used for PANI and PPy [33]. For this reason, it was the selected as candidate for this study. In this way, the polyelectrolyte complex formed by colloidal particles made of a conductive insoluble core surrounded by PSS polyanion and generating a hydrophilic shell made possible to obtain a printable ink formulation soluble in water [42]. In addition, the tunability of secondary doping has long played a role in studies of conjugated polymers because it can increase the conductivity and improve carrier injection at electrodes enhancing sensors performance. Unlike the reversal change in conductivity by primary doping/de-doping, this process promotes an irreversible modification of the electrical conductivity even upon removal of the secondary dopant. High values of electrical conductivity can be achieved by the so-called secondary doping. During the treatment with different solvents [51–55], the band structure of PEDOT:PSS drastically changes because there are electrons that have been removed. As a consequence, polarons and spinless bipolarons, which are oxidized states of the PEDOT unit responsible of the charge carrier concentration and thus of the electrical conductivity, will form introducing energy states between the lowest unoccupied molecular orbital (LUMO) and the highest occupied molecular orbital (HOMO) [50,56]. MacDiarmid and Epstein [57] noticed that a post treatment of primary doped PANI samples led to a change in the molecular conformation from “compact coil” to “expanded coil”, enhancing the conductivity. Similarly, Kim et al. [58] reported in 2002 a comparable improvement in conductivity in PEDOT:PSS films by a change of solvents of dimethyl sulfoxide (DMSO), N,N-dimethyl formamide (DMF), and tetrahydrofuran (THF) [59]. Nevertheless, the literature misses to describe the effects of post-treatments on PEDOT:PSS that can be easily correlated to gas sensing performance or selectivity tunability. For this reason, this study aims at gaining a better understanding of these effects on PEDOT:PSS, establishing relationships amid different post-treatments compared to the chemical and physical properties of the material and the sensing response of the ink-jet printed devices. For this purpose, ink-jet printed sensors with pristine PEDOT:PSS were obtained and the effect of different secondary doping post fabrication treatments on the devices were studied. MeOH and H_2SO_4 were used as one-electron oxidants sufficiently strong to transfer holes to the transport levels of the PEDOT:PSS, altering the band structure by introducing polaronic states in between the band gap. Finally, the evaluation of sensing response at different temperature towards a low concentrations range of VOCs vapors up to 5% of the saturated vapor pressure, 10 ppm of NO_2 and up to 10% of relative humidity (RH) by means of a proper characterization system were studied on the fabricated devices along with their initial long-term stability and repeatability. The obtained results provide encouraging knowledge to develop electronic nose systems with a potential wide range of analytes detection.

2. EXPERIMENTAL

2.1 Materials

The poly(3,4-ethylenedioxythiophene) polystyrene sulfonate (PEDOT:PSS) aqueous solution (Clevios™ PH1000) was purchased from Heraeus (Leverkusen, Germany) with a solid concentration of 1.0–1.3 wt% and a ratio of 1:2.5. Acetone (ACS reagent grade, ≥99.5%), ethanol (EtOH) (Analytical standard for GC, ≥99.9%), 2-propanol (IPA) (ACS reagent grade, ≥99.8%), ammonium hydroxide solution ($NH_3 \cdot H_2O$) (ACS reagent grade, 28.0-30.0 wt% NH_3 basis), methanol (MeOH) (Anhydrous, 99.8%) and sulfuric acid (H_2SO_4) (ACS reagent grade, 95.0-98.0%) were purchased from Sigma-Aldrich (Milano, Italy). Common household bleach based on sodium hypochlorite (NaClO) (Solution with 2.2 wt%) was employed. Two tanks of O_2 and a mixture of nitrogen and NO_2 in the concentration of 25 ppm were supplied by Linde Gas. All the chemicals were used as received without further purification. Deionized water (DI water) was obtained from a reverse osmosis (RO) purification system. Si 4'' wafers finished with a 1 µm thick thermally grown SiO_2 layer were purchased from Si-Mat (Kaufering, Germany) and used as a substrate for the chips fabrication.

2.2 Substrate preparation

The substrate was developed by using standard clean room processes (Figure 1a) starting from 4'', single side polished, P type, (100) Si wafers (resistivity 1–10 Ω·cm) finished with 1 µm thermal SiO_2. A 10 nm thin layer of Ti was evaporated in order to promote the adhesion of the following 100 nm of Au that ensures the contact. Contact pads and electrodes (Figure 1b) were patterned by UV photolithography through a photomask and then wet-etched. The two fingers are 7 mm long and 250 µm wide with a gap of 200 µm. The length and width of a single contact pad are 1 mm and 2 mm respectively.

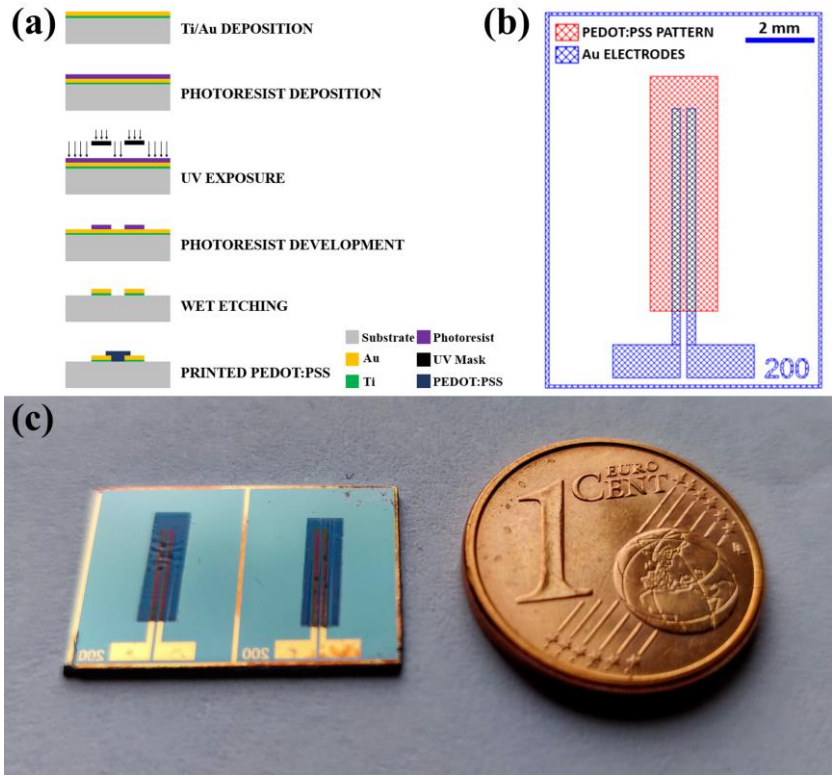

Figure 1: (a) Sketch of the fabrication steps used to produce the gas sensor (b) Layout of the device: red layer is the pattern of the ink-jet printed PEDOT:PSS film, while blue layer corresponds to the contact pads and electrodes (c) Picture of the fabricated PEDOT:PSS gas sensors.

2.3 Conductive ink preparation

The typical ink formulation was prepared following a two steps process using pristine Clevios™ PH1000. In the former, the PEDOT:PSS aqueous dispersion underwent a sonication treatment by means of a digital sonifier Branson SFX 250 (Danbury, U.S.A.), operating in pulse mode for 20 minutes at the 50% of the maximum power and cooled down in an ice water jacket. The latter is a filtering step. The sonicated solution was double filtered by means of a syringe connected to a disposable filter with a pore size of 0.45 μm. Such two steps preparation is necessary because it ensures a better dispersion, the right viscosity range (0.5 – 40 mPa·s) for the printing process and it ensures that the residual particulate in the conductive ink is smaller than 1% of the diameter of the printer's nozzle, avoiding the occlusion/clogging of the nozzle and providing good repeatability and printing performance.

2.4 Device fabrication by Ink-Jet printing

After an O_2 plasma activation of the substrate's surface for 15 minutes with a Diener Atto Plasma System (Ebhausen, Germany), the PEDOT:PSS formulation was ink-jet printed onto the electrodes to obtain a 2x7 mm^2 film from a digital model. The employed jet printer is a piezoelectric drop-on-demand (DOD) Jetlab 4 supplied by MicroFab (Texas, U.S.A.). The conductive ink was loaded in the

reservoir, the jetting was regulated and observed from the lateral camera and then the printing was started. All the parameters were set as well described in details in the optimization printing process reported in [60]. The flow velocity was fixed at 4 mm/s, the back pressure set at -8 psi, the frequency selected at 550 Hz; a W-shaped wave was exploited with a dwell time of 3 µs and a maximum positive voltage of 65 V. The PEDOT:PSS was then annealed on a hotplate at 120 °C for 10 minutes. The sensors, used as prepared, were compared with the treated ones in a MeOH bath or in a H_2SO_4 one at different concentrations. After the post-treatment, the devices were rinsed in DI water and dried on a hotplate for 3 minutes at 120 ºC.

2.5 Characterization

2.5.1 FTIR

FTIR analyses were performed in transmission mode in order to evaluate the chemical composition. The experiments were conducted on dried samples by means of a Thermo Scientific Nicolet iS50 FTIR Spectrometer (Milano, Italy). The solutions were analyzed after being applied onto a silicon wafer before and after the MeOH and H_2SO_4 treatments. The analysis was carried out with a resolution of 4 cm^{-1} and samples were scanned 32 times in the wavenumber range between 650 and 4000 cm^{-1}. A background measurement was performed on all samples prior to FT-IR analysis. The results were acquired and evaluated using the Omnic software.

2.5.2 Contact Angle

Contact angle measurements were performed on a Kruss DSA10 instrument (Hamburg, Germany), equipped with a digital camera and an image analyzer. Analyses were performed at room temperature by means of the sessile drop technique. Five to eight measurements were acquired on each sample and the mean values estimated. The measuring liquid was distilled water (γ=72.1 mNm^{-1}).

2.5.3 Profilometer

The polymer films thickness and roughness were measured with a KLA Tencor P10 surface stylus profiler (California, U.S.A.). Multiple measurements were performed on each sample before and after the post-treatments and the mean values were estimated.

2.5.4 Sensing Setup

Figure 2 shows the custom-made experimental setup used to retrieve the PEDOT:PSS sensing responses [61].

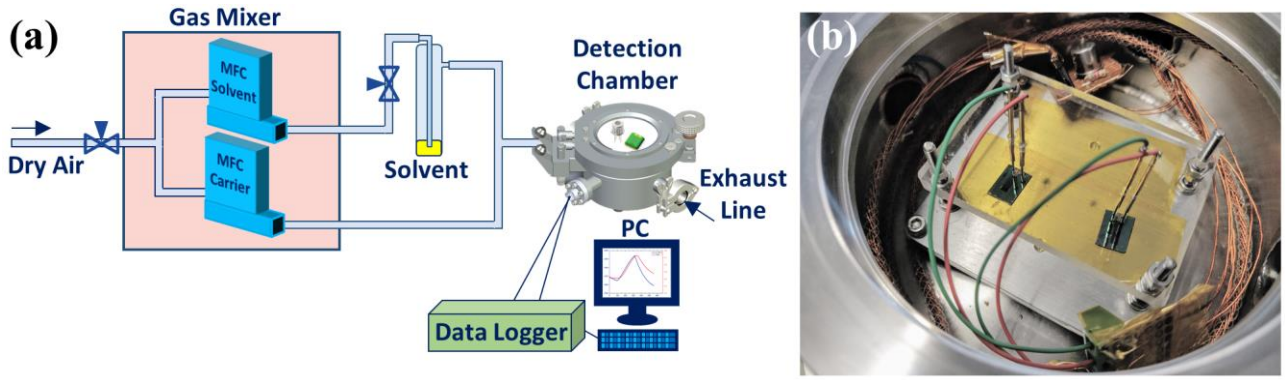

Figure 2: (a) Scheme of the experimental sensing setup used to perform gas sensing measurements (b) Interior of the gas detection chamber.

More in detail, in order to produce and deliver selected concentrations of solvent vapors to the samples, a custom-built sensing setup was exploited for the real-time characterizations. In the system, a stream of oil-free dry air (DA) is exploited as carrier and diluting gas. The main stream is divided and regulated into two fluxes inside an Environics Gas Mixing System (series 4000) equipped with two mass flow controllers (MFC) and controlled by a dedicated software for the mass flow regulation. The DA flows through a bubbler properly filled with the volatile organic compound (VOC) to be tested, producing its saturated vapor. Then, the two flows are recombined, mixed, and directed to a detection chamber made of a stainless-steel assembly with a 100 mm inner diameter. There exists a latency period from the opening time of the valve and moment in which the vapor fills the chamber and can be detected. This delay affects the response and recovery time. The operational temperature for the sensing measurements herein reported is 21 °C and it was measured with a PT1000 sensor. In order to evaluate the effect of the temperature on the gas sensor, a Supercool Peltier thermoelectric module is installed beneath the sample holder platform inside the sensing chamber and bonded to a machined aluminium heat sink for heat transfer. In this way, it is possible to modulate the operational temperature, cooling down to 10 °C and heating up to 60 °C by applying different current values. In addition, a Figaro TGS2600 sensor is placed inside the sensing chamber and it is used as a reference in order to validate the whole sensing setup. 200 sccm of DA were set to flow on the samples. All the experiments carried out in this work exploited six different liquid analytes, namely acetone, EtOH, IPA, NaClO solution (testing chlorine-based vapor), NH_4OH solution (testing NH_3 vapor), H_2O and two gases, O_2 and NO_2.

2.5.5 Sensing Analyses

The electrical resistance was investigated by using two-probes measurements, exploiting a data acquisition unit 34970A supplied by Keysight (Milano, Italy). In the DC analysis, a voltage was applied between the electrodes and the current was measured, acquiring directly the resistance as a

function of the time. For each test, dry air was introduced for 120 s in order to get the baseline. Successively, the sensor was exposed to the analyte at the desired concentration for 300 s, followed by further 300 s that was set as recovery time. Initial long-term stability measurements were carried out over a period of almost 2 hours, repeating 12 times the gas sensing cycle.

The typical response of the sensor to a particular gas (S) is calculated as the ratio between the steady-state resistance variation ΔR and the baseline resistance of the device (Eq. 1):

$$S = \frac{\Delta R}{R_{Baseline}} \qquad \text{(Equation 1)}$$

In this work, the formula used is reported below (Eq. 2):

$$S\% = 1 - \frac{R_{Gas}}{R_{Baseline}} \times 100 \qquad \text{(Equation 2)}$$

O_2 and NO_2 fluxes were regulated using dry air as diluting gas in order to obtain the requested concentrations; while saturated vapors of the VOCs were extracted by bubbling dry air through the bubbler. The concentration of the volatile vapor is expressed as a percentage obtained from the ratio between the saturated vapor flow coming out of the bubbler and divided by the total flow reaching the detection chamber, using the following equation (Eq. 3):

$$\mathcal{C}(\text{Saturated vapor }\%) = \left(\frac{P^*}{P} \times \frac{f}{f+F}\right) \times 100 \qquad \text{(Equation 3)}$$

where P is the input air pressure (atmospheric pressure in this case), P* is the saturated partial pressure of the analyte, f and F are the mass flow rate of MFC of the pure dry air and MFC of the carrier respectively. P* is calculated by Antoine's equation (Eq. 4) as a function of the temperature and Antoine's component-specific constants A, B and C [39,62–64]:

$$P^* = 10^{\left(A - \frac{B}{C+T}\right)} \qquad \text{(Equation 4)}$$

At room temperature the saturated vapor pressures of acetone, ethanol, IPA, NaClO, NH_3 and H_2O are 0.254 atm, 0.061 atm, 0.045 atm, 0.020 atm, 0.732 atm and 0.0245 atm respectively. More in detail, in order to evaluate the contribution of NH_3 vapor from NH_4OH liquid solution, it was assumed negligible the humidity due to the presence of water molecules. In fact, at 21 °C the partial vapor pressures of NH_3 and H_2O of a 30% NH_3 aqueous solution are 0.732 atm and 0.017 atm respectively [62,65]. Hence, the molar fraction of NH_3 is 97.7%.

Sensing measurements at 10 °C, 20 °C, 30 °C, 40 °C, 50 °C and 60 °C were carried out by exploiting a Peltier module and changing the current between 0.2 A and 2 A through a power supply, using a PT1000 sensor as a temperature reference.

3. RESULTS AND DISCUSSION

As a first step, in order to evaluate the effects of doping, ink-jet printed sensors with pristine PEDOT:PSS were prepared and, for some of them, the already coated film was immersed in secondary doping solutions and then dried. MeOH and H_2SO_4 were used as one-electron oxidants sufficiently strong to transfer holes to the transport levels of the PEDOT:PSS structure and alter its band gap. This process led to an enhancement in conductivity from 0.5 S/cm of the untreated sample to 1021 S/cm for the treated ones, reducing significantly the energy barrier for the intra-grain and inter-domain charge hopping. The resistances of the PEDOT:PSS films were evaluated and are summarized in Table 1. Both charge-carriers mobility and carrier density were affected by doping [3]. We observed a significant drop in resistance of three orders of magnitude for the films treated with H_2SO_4 and two for the ones doped with MeOH. By diluting the H_2SO_4 with different ratios and controlling the dipping time, the change in resistance is less pronounced because the doping level is lower. In this way, it is possible to modulate the oxidation level. All the films showed a good stability concerning the conductivity. Indeed, no appreciable variations were observed after 10 months.

Table 1: Resistance values for the PEDOT:PSS films before and after the post-treatment with MeOH and several concentrations of H_2SO_4.

Post-Treatment	**Resistance**	
	Untreated Film	**Treated Film**
PEDOT:PSS + MeOH	22.52 kΩ	1221 Ω
PEDOT:PSS + H_2SO_4	9.75 kΩ	10 Ω
PEDOT:PSS + H_2SO_4:H_2O 2:1	9.42 kΩ	20 Ω
PEDOT:PSS + H_2SO_4:H_2O 1:1	9.75 kΩ	85 Ω
PEDOT:PSS + H_2SO_4:H_2O 1:2	13.67 kΩ	200 Ω
PEDOT:PSS + H_2SO_4:H_2O 1:4	14.18 kΩ	900 Ω

Figure 3(a) shows the PEDOT:PSS film printed on top of the electrodes. The thin film appears homogeneous and it is possible to notice the regular stripes of the ink-jet printer. There are no satellites during the printing process and, after an O_2 plasma treatment, the wettability is enhanced both on the gold and on the silicon. As a consequence of the dipping treatment, the thickness of PEDOT:PSS films changed as illustrated in Figure 3(b). The pristine PEDOT:PSS thin film has a thickness of 655 nm, while it is significantly reduced to 500 nm after the post-treatment with MeOH and 403 nm after H_2SO_4 doping. For the MeOH treatment, the reduction is less pronounced.

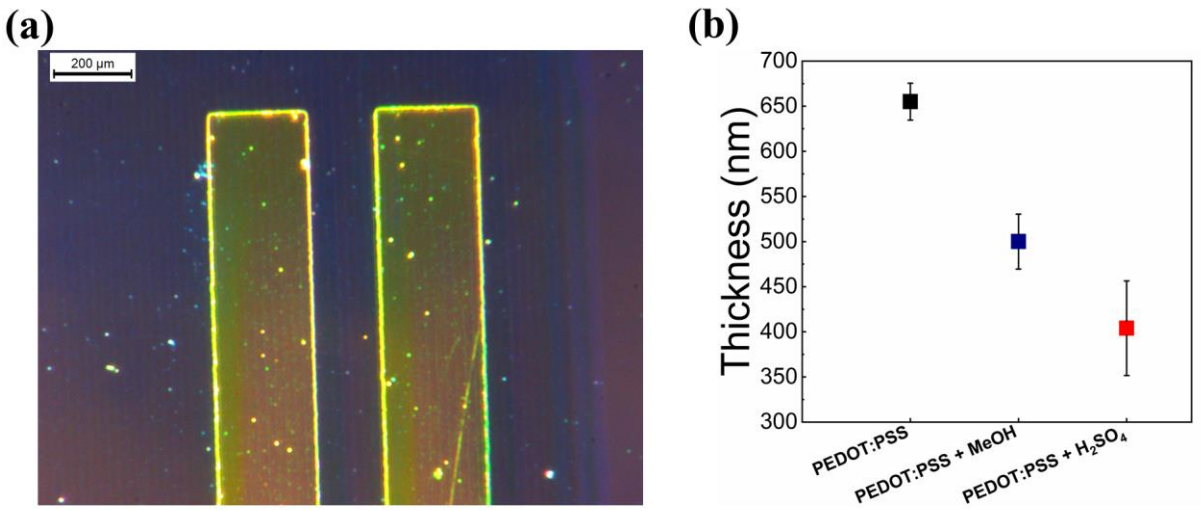

Figure 3: (a) Optical image of PEDOT:PSS thin film ink-jet printed on top of gold electrodes (b) Comparison of the thickness of pristine, H_2SO_4 – doped and MeOH – treated PEDOT:PSS films.

In order to explain the experimental evidence, it is worth analyzing the PEDOT:PSS structure and its functionality, from the atomistic point of view all the way to its macroscopic dimensions. In fact, pristine PEDOT is typically insoluble, the chains are in a natural disorder in the so-called random coil configuration and, in its neutral state, appears unstable with a peculiar pale bluish color [5]. However, when dispersion polymerized with the polyanion poly(4-styrenesulfonate) (PSS), a colloidal water-soluble solution is achieved. The polyelectrolyte complex is formed by nanoparticles where the PEDOT inner core is hydrophobic and conductive, while the outer shell is formed by PSS chains that are hydrophilic and insulating. Those nanoparticles are dispersed in an amorphous region formed by non-stochiometric excess of PSS. This polymer blend has proven to be a stable formulation for the printing process also due to its viscosity in the range of 0.5 – 40 mPa·s [42]. In this system, PEDOT is already primary doped and in its oxidized state. In fact, about one third of the monomers on the chain has been oxidized [66]. The effect of secondary doping through the post-treatment can be explained by a change in morphology [67–69] and to a small extent by a modification of the oxidation level of the conducting polymer. The reduction in thickness is related to a screening effect by the dopant that facilitates a phase separation of PEDOT and PSS, leading to a better interconnection between the conducting PEDOT domains through the film [66]. Furthermore, it implies an enhancement of volumetric capacitance and, consequently, its attitude at implementing an efficient electrochemical activity in presence of oxidizing/reducing agents. During the secondary doping there is a removal of the PSS that is likely washed away from the surface during the process. In fact, in water H_2SO_4 dissociates into H^+ and HSO_4^-. During the post-treatment, the proton released by the acid will interact with the PSS^- counter anion. The reaction can be summarized as $H_2SO_4 + PSS^- \rightarrow HSO_4^- + PSSH$ [70–72]. In this way, the enhancement in conductivity after the H_2SO_4 treatment is attributed to the fact that the non-conductive anions of some PSS^- were substituted by the conductive

anions of HSO_4^-. While for the other doping with MeOH, even though there isn't an ionic substitution, the polar hydrophilic alcohol with a high dielectric constant still induces the screening effect and the solvation process of the PSS between counter ions and charge carriers, which reduces the Coulomb interaction between positively charged PEDOT and negatively charged PSS [51,73]. For this reason, the segregated hydrophilic PSS can be easily removed from the surface of the film after the treatment with MeOH. In both secondary doping post-treatments, from the morphological point of view, the configuration changes from random coil to a more linear structure, presumably due to the employment of small-sized, less steric counter-ions (Figure 5b) [51,66,67,74]. Hence, it promotes a better interaction between different polymer chains, allowing an easier hopping charge transfer and further delocalizing the positive charges. The doped films present a more oriented system where the linearization of the chains allows the generation of crystallites of π-π stacked chains embedded into amorphous regions of less ordered chains. During the linearization of the chains, PEDOT backbones undergo a transition from the aromatic to quinoid state in the region where the polarons are localized due to a change in the bond length [3]. In this way, carrier transport involves hopping of the charge carriers from one site to another within a manifold of transport levels that are relatively close to one another both energetically and spatially. Therefore, the combined effects of chain linearization, increased doping level through further oxidation, removal of insulating polymers, and resulting morphological change are considered to give rise to the enhanced conductivity of PEDOT:PSS system by secondary doping post-treatments. It has to be underlined that the doping process is very quick and the change in conductivity happens with a short treatment time for both solutions.

As a support for this evaluation, water contact angle measurements were performed, and the results are summarized in Figure 4.

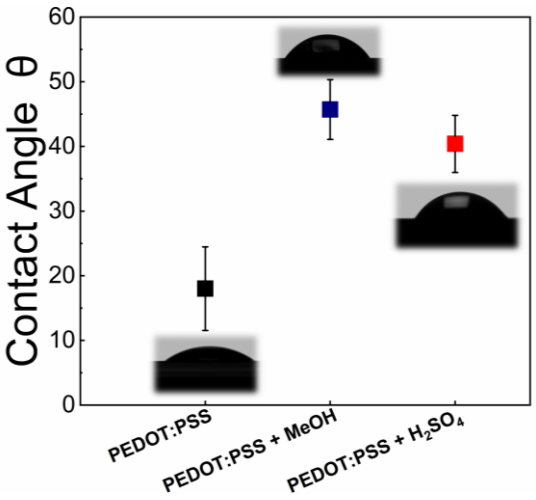

Figure 4: Comparison of the contact angles of pristine, H_2SO_4 – doped and MeOH – treated PEDOT:PSS films.

A significant difference in surface properties is appreciable before and after the secondary doping. The contact angle of pristine PEDOT:PSS is around 18 degrees. This is coherent with the core-shell structure where the highly hydrophilic PSS rich region is in the external part exposed to the film surface, while the hydrophobic PEDOT chains are in the core. The PSS presence allows a good water dispersion and the wettability results to be very good with a low contact angle. On the contrary, after the treatment in H_2SO_4 and MeOH, the wettability was reduced. Contact angles were 40 and 46 degrees respectively. This is due to the intrinsic property of PEDOT that is hardly soluble in water. After the secondary doping, part of the PSS was washed away and a separation process happened, letting part of the PEDOT molecules to be exposed on the surface.

Figure 5(a) shows the chemical structure of PEDOT:PSS with their interactions. FTIR spectroscopy was undertaken to explore the chemical environment of PEDOT:PSS thin films before and after secondary doping, trying to explain the de-sulfonation of PSS (Figure 5c).

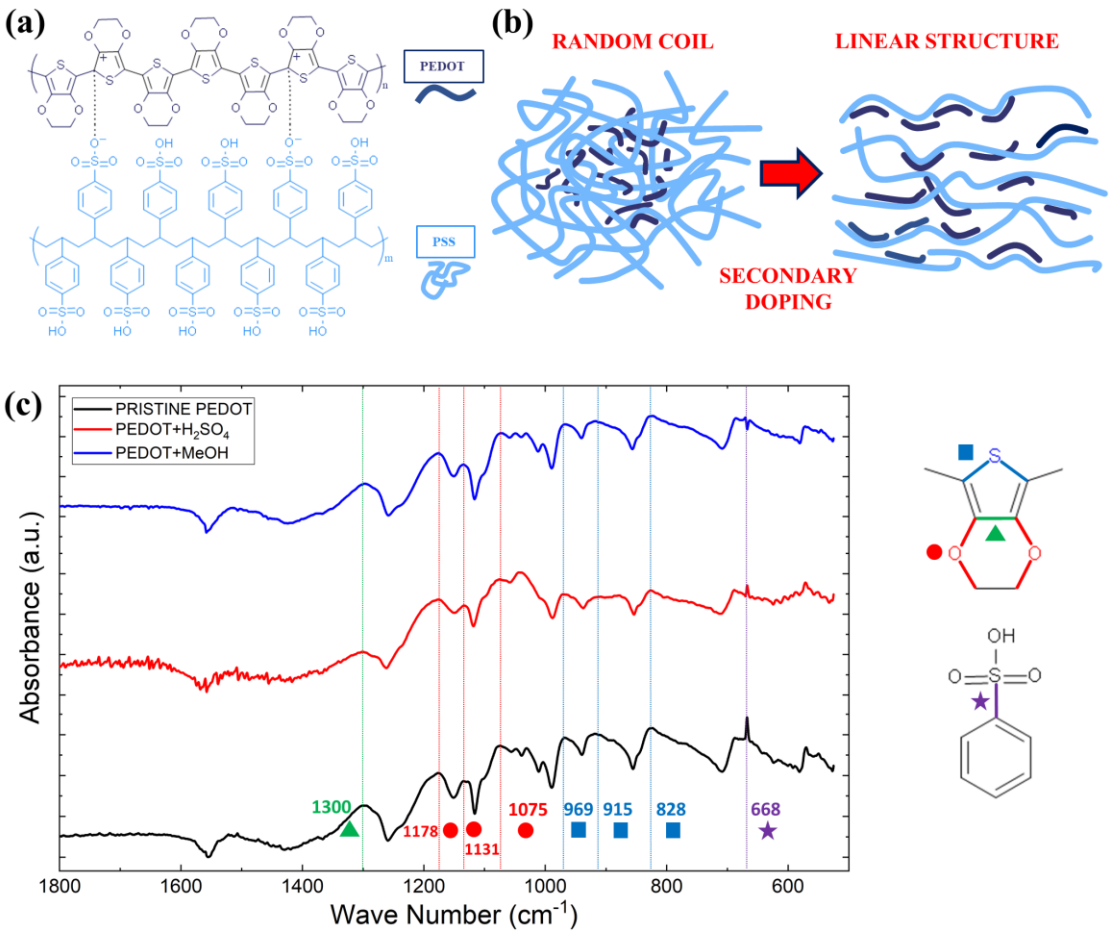

Figure 5: (a) PEDOT:PSS polyelectrolyte complex structure (b) Sketch of the structural rearrangement of PEDOT:PSS from random coil to a linear structure (c) Transmission FTIR spectra of pristine, H_2SO_4 post treated and MeOH doped PEDOT:PSS thin films.

The main characteristic PEDOT:PSS IR peaks were identified. The vibrations at 828, 915 and 969 cm^{-1} are assigned to the PEDOT C-S bonds in thiophene rings [75,76]. The stretching mode of the C-O-C bonds can be seen at 1075, 1131 and 1178 cm^{-1}. The vibration at 1300 cm^{-1} can be attributed to

the C-C asymmetric stretching mode of the quinoid structure in thiophene rings. The peaks near 600 cm^{-1} are assigned to the sulfate ions with the S-O stretching [70]. This band is absent in the pristine PEDOT:PSS film, while it appears on the H_2SO_4 treated spectrum. This indicates that some sulfate ions SO_4^{2-} remain in the PEDOT:PSS film after the secondary doping, even after a precise rinse in deionized water. It is very likely that some PSS undergoes de-sulfonation process and ion substitution. The impact of acid post-treatment also affects the band at 668 cm^{-1}. This peak has been debatably attributed to the PSS C-S bond [77]. It can be seen that its intensity is reduced after the H_2SO_4 post-treatment. This may be explained with the removal of some PSS, leaving PEDOT stacks free of it. This is in agreement with the results observed by Kim *et al* during their spectroscopy analysis [78].

Three different types of devices described in the aforementioned section were selected to be tested in their sensing behavior as chemiresistors towards eight different analytes at room temperature, following the protocol reported in the experimental part. Various vapors and gases were investigated starting either from the liquid, including one ketone (acetone), two alcohols (EtOH and IPA), common bleach based on NaClO, NH_3 molecules from NH_4OH solution, H_2O vapor (RH from 0% to 10% at 21 °C) or fluxing directly two oxidizing gases: O_2 and NO_2. These VOCs were selected because of their different chemical and physical properties like chain length and functional groups. The gas concentrations for real time exposure are reported in percentage respect to the saturation vapor pressures. Figure 6 displays the dynamic sensing curves of the three different PEDOT:PSS systems exposed to an oxidizing gas (top) and towards a reducing vapor like acetone (bottom). The resistance is expressed as a function of time and the green curves are related to a commercial MOS sensor (Figaro TGS 2600) that has been used as a reference. Differently from the MOS sensors, they manage to properly operate at room temperature, without the need of a heating element, which represents a clear advantage from the point of view of power consumption, making them suitable for flammable or explosive environments or portable detection systems. By observing the reported curves, it is possible to state that the drift of the resistance is almost negligible and all the times the sensor recovered to the original value of the steady state baseline. Only in the case of ammonia vapor the recovery was incomplete within the time scale of the experiment. An encouraging result is the response time. In all the carried out experiments, the sensors made with PEDOT:PSS always had a faster response compared to the commercial Figaro TGS 2600, sensing the different gases earlier. The faster response and recovery may be due to high diffusion and deep penetration of the gas molecules on the very smooth surface of the sensing film. The response time was estimated to be in the range of few hundreds seconds that is a good achievement with respect to the time found in other manuscripts. In good agreement with the literature, the electrical resistance of our sensors made with

pristine PEDOT:PSS and the one doped with MeOH significantly increased when exposed to all the VOCs, while it sharply decreased when in contact with oxygen.

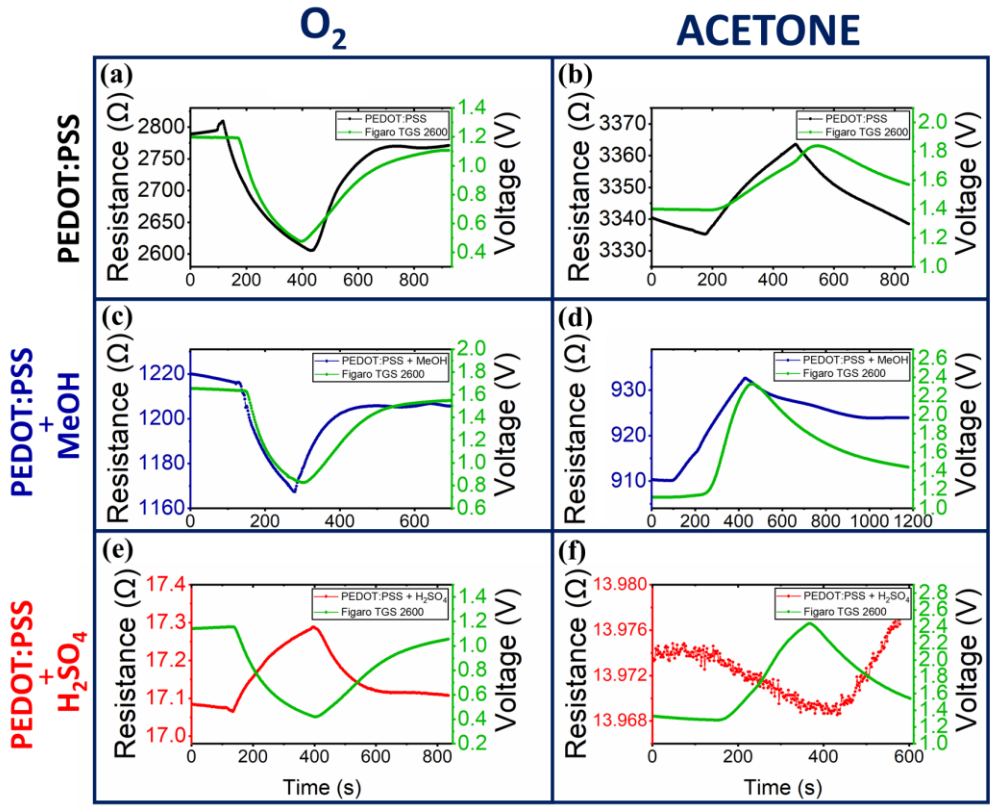

Figure 6: (a) Dynamic sensing response of pristine PEDOT:PSS sensor towards oxygen; (b) Sensing response of pristine PEDOT:PSS sensor towards acetone; (c) Sensing response of PEDOT:PSS MeOH doped sensor towards oxygen; (d) Sensing response of PEDOT:PSS MeOH doped sensor towards acetone; (e) Sensing response of PEDOT:PSS H_2SO_4 doped sensor towards oxygen; (f) Sensing response of PEDOT:PSS H_2SO_4 doped sensor towards acetone.

This behavior is correct because PEDOT:PSS is a p-type material where the main charge carriers are holes. Different changes in resistances are related to the nature of the gas/vapor. When the sensor is exposed to a reducing gas, the polymer loses some electrons. Therefore, the resistance will drop because more holes are able to contribute to the conductivity. Instead, an oxidizing gas, reducing itself, oxides the material that gains some electrons. In this case, the resistance will increase. The doping of the material by the analyte is a reversible process, while the secondary doping is irreversible. When the gas is gone, the polymeric film will de-dope and the resistance returns to the initial value. In contrast, the sensor doped with concentrated H_2SO_4 (third row) shows an atypical behavior for a p-type sensor: the resistance increased after the oxygen exposure and decreased when acetone vapor was flowed.

The sensing results (Figure 7) demonstrate the effect of doping on gas response with respect to the different VOCs analytes at a fixed concentration of 5% of saturated vapor. It appears that the post-treatment with MeOH increased the sensing response by a factor 2 or more with respect to the pristine PEDOT:PSS towards all gases except ammonia and oxygen. While the treatment with concentrated H_2SO_4 was always detrimental. With this post-treatment the conductivity had the best enhancement

and we observed an inversion of behavior never found in the literature before. A possible explanation is that the concentrated H_2SO_4 is too strong as a dopant and some partial over-doping reactions occur, compromising the electrical response with respect to the pristine system. This over-doping effect slightly deteriorates the electrical conductivity of the device after a critical value [79,80]. This effect, where the curve of conductivity as a function of the doping shows a maximum, was already observed for PEDOT:PSS [70]. In addition, it can be seen that the pristine PEDOT:PSS shows relatively high response towards NH_3 compared with the other VOCs and the secondary doping seems not to improve the gas sensing response towards this gas.

The next step was a study on the dilution of H_2SO_4 as doping bath. Figure 7(b) shows that the gas response increased as the concentration of H_2SO_4 used for the post-treatment decreased. The doping with 1:4 H_2SO_4 dilution displayed the best performance towards all gases except NH_3. In fact, the sensing response was higher than the pristine PEDOT:PSS sensor and, in some cases, even higher than the sensor doped with MeOH. It was possible to notice that up to 2:1 H_2SO_4 dilution the sensor showed the atypical behavior, while starting from 1:1 dilution the curves where coherent with the pristine and MeOH doped sensors with a higher response as the dilution increased.

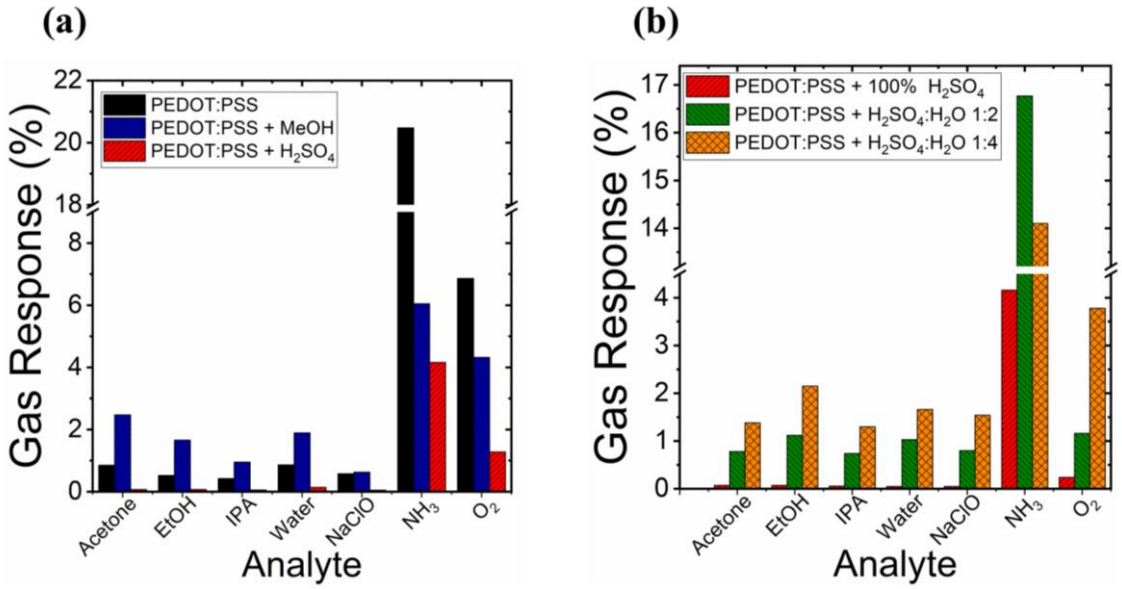

Figure 7: (a) Sensing response of pristine PEDOT:PSS, PEDOT:PSS H_2SO_4 doped and PEDOT:PSS MeOH doped sensor towards different analytes at a fixed concentration of 5% of saturated vapor (100% for oxygen due to setup limitations) at room temperature. (b) Sensing response of PEDOT:PSS sensor doped with different H_2SO_4 concentrations towards various analytes at a fixed concentration of 5% of saturated vapor (100% for oxygen due to setup limitations) at room temperature. The breaks were inserted to illustrate the relative sensing response of most of the vapors.

Figure 8 reports the trend towards the VOCs analytes at different concentrations. As a general behavior, the gas sensing response grows monotonically with the vapor concentration. In addition, all the sensors exhibited a remarkably high affinity towards NH_3 among all of the tested VOCs, while a very tiny responsive signal was observed with NaClO and IPA. Moreover, these devices are more sensitive towards the amines functional group that has an electron lone pair. When sensors are

impinged with an electron donating gas like ammonia, the depletion of holes from the valence band of PEDOT:PSS occurs resulting in a significant increase in resistance with a sensing response in the range of 14-20%. This result suggests PEDOT:PSS as a good candidate for the detection of NH_3 and its derivatives.

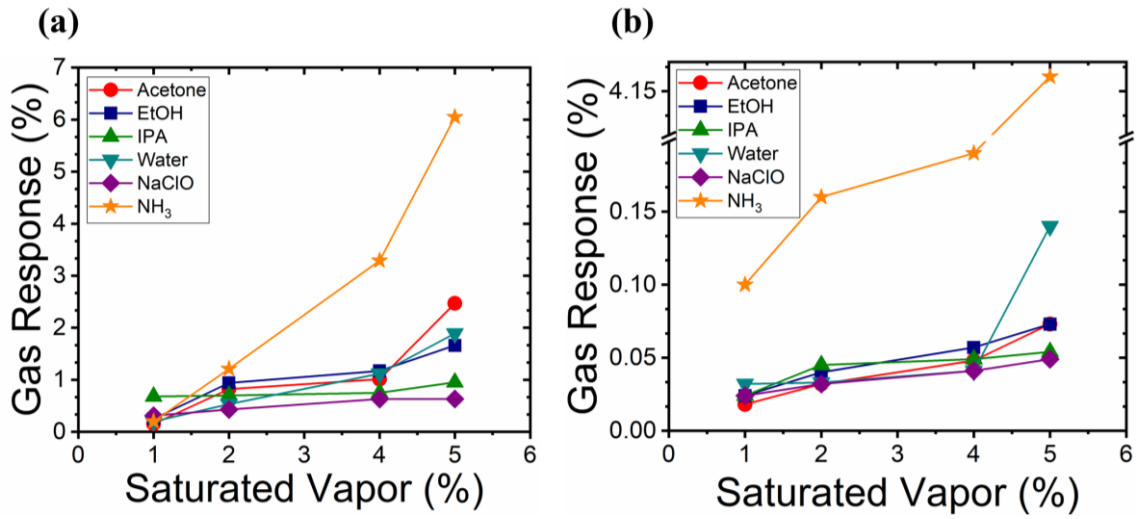

Figure 8: (a) Gas sensing response as a function of gas content for the different tested gas analytes at room temperature for PEDOT:PSS doped with MeOH; (b) Gas sensing response as a function of gas content for the different tested gas analytes at room temperature for PEDOT:PSS doped with H_2SO_4. The analytes concentration is reported in percent of their saturated partial vapor pressure.

The actual lower detection limit is under further investigation due to long bubbler retention times at low partial pressures. In the present work we tested VOCs concentrations as low as 2% of the saturated vapor pressure with a readable sensing response. Based on the current results we expect to detect even lower concentrations of the VOCs and also be able to detect other analytes of interest.

Another study has been carried out investigating the effects of NO_2 on the fabricated chemiresistive gas sensors, revealing a strong influence on the active materials. Figure 9 shows the general response of the pristine PEDOT:PSS and their respective post-treatments thin films to 10 ppm NO_2 gas at room temperature. NO_2 is known to be a highly active and electron donating free radical. All sensors were highly affected by the release of the gas inside the chamber with an immediate increase until the saturation of the electrical resistance due to the electron transfer from NO_2 to the partially positive charged sulfur site on the backbone of the p-type PEDOT:PSS sensors; while the device doped with pure H_2SO_4 still maintained the opposite trend behavior as it was observed previously. All of them fully recovered to the original baseline except the pure H_2SO_4 doped one. Evaluating the sensing responses, it is possible to notice the beneficial secondary doping of MeOH leading with a 29% response respect to the pristine one and the sensor doped with diluted H_2SO_4 with 21% and 17% respectively. Much lower was the response of the pure H_2SO_4 doped sensor. Compared to the other VOCs analytes, it appears that all the tested devices have better performances with the same trend in

the gas sensing response. This strong influence of this abundant gas in the atmosphere can potentially introduce on the market PEDOT:PSS devices with different doping as great candidate for the NO_x detection in air quality monitoring.

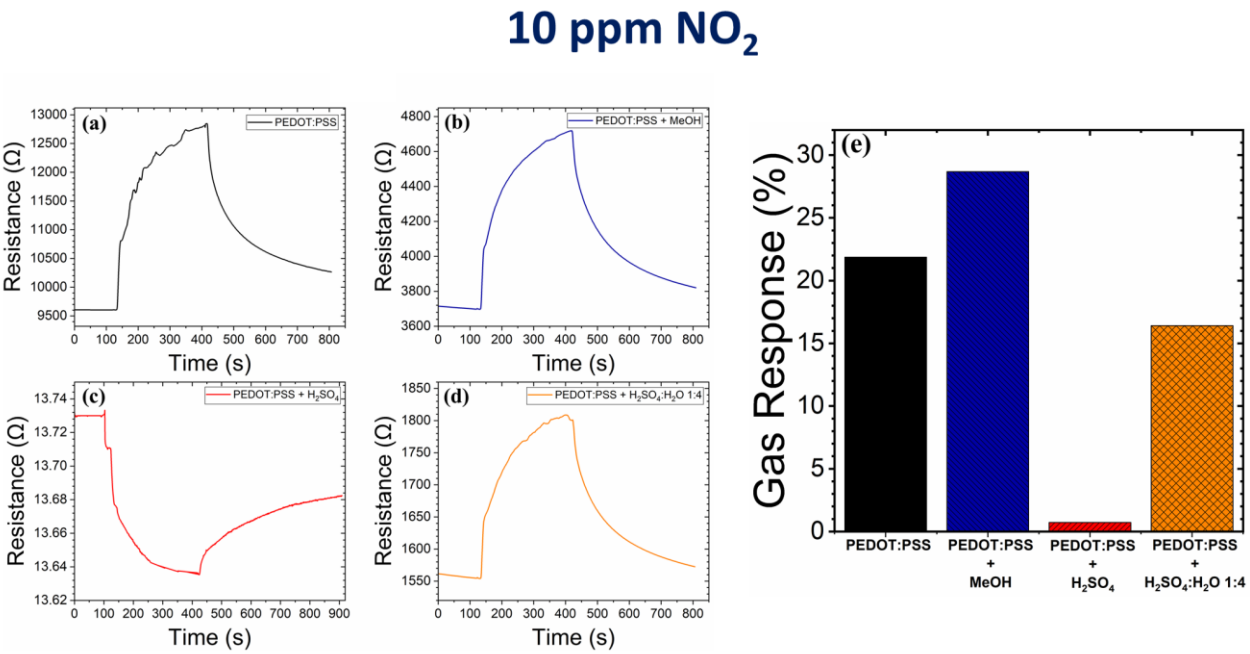

Figure 9: Dynamic Sensing curves of (a) PEDOT:PSS sensor, (b) PEDOT:PSS MeOH doped sensor, (c) and (d) PEDOT:PSS doped with different concentrations of H_2SO_4, and (e) gas sensing response towards 10 ppm of NO_2.

In addition, long-term stability was tested and there were some fluctuations regarding the baseline resistance and the sensing response as shown in Table 2 and Figure 10. More precisely, the electrical resistance generally increased in ambient air over a period of 10 months in different ways. After 6 months, films doped with H_2SO_4 presented a variation up to 10%, while after 10 months it increased of up to 30% and 53% for the 1:4 dilution respect to the original values. The same trend was observed for the pristine PEDOT:PSS: 6% and 25% respectively. Sensors doped with MeOH showed a much higher change with a variation of 43% and 178% respectively. It is worth noting that when placing the devices in the sensing chamber and fluxing dry air, the resistance decreased, reducing the variation and approaching to a new baseline stabilization without further abrupt fluctuations.

Table 2: Resistance values for PEDOT:PSS films with different post-treatments after 6 and 10 months.

Post-Treatment	**Resistance**		
	t=0	**t=6 months**	**t=10 months**
PRISTINE PEDOT:PSS	10.6 kΩ	11.3 kΩ	13.2 kΩ
PEDOT:PSS + MeOH	1221 Ω	1657 Ω	3390 Ω
PEDOT:PSS + H_2SO_4	10 Ω	11 Ω	13 Ω
PEDOT:PSS + H_2SO_4 :H_2O 2:1	20 Ω	21 Ω	23 Ω

PEDOT:PSS + H_2SO_4:H_2O 1:1	85 Ω	93 Ω	112 Ω
PEDOT:PSS + H_2SO_4:H_2O 1:2	200 Ω	213 Ω	292 Ω
PEDOT:PSS + H_2SO_4:H_2O 1:4	900 Ω	949 Ω	1380 Ω

Moreover, Figure 10(a) compares the sensing response after 10 months. The very same devices were able to detect the analytes and recover, maintaining their performance with a slight reduction of gas response that could be due to environmental effects. This result allows utilizing these sensors multiple times over a long period of time.

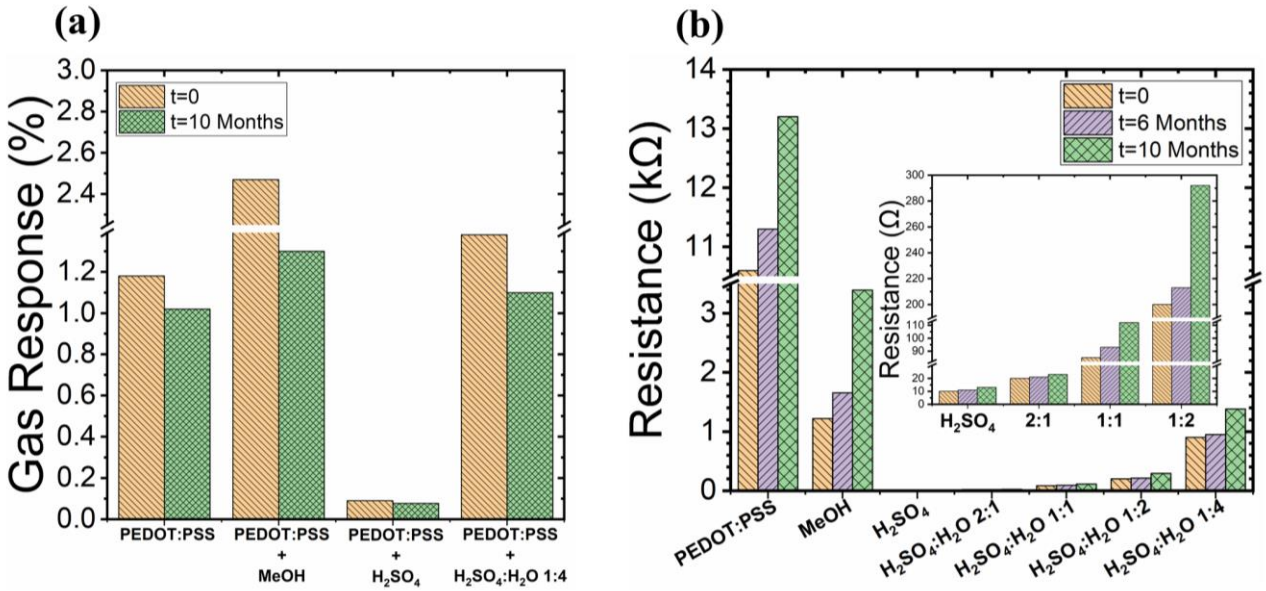

Figure 10: (a) Gas sensing response towards acetone at a fixed concentration of 5% of saturated vapor at room temperature before and after 10 months, (b) behavior of the baseline resistance of PEDOT:PSS with different secondary doping in ambient air as a function of time. The inset magnifies low resistance values in the range of 0-300 Ω.

Furthermore, 12 consecutive cycles were performed over a period of almost 2 hours in order to evaluate the initial long-term stability of the different electronic devices and the repeatability of the measurements. Figure 11 shows an example of the responses towards acetone at 5% of the saturated vapor. As expected, all the films behave with an increase of the electrical resistance, while the one post treated with concentrated H_2SO_4 showed the inverted behavior. All the cycles presented almost the same sensitivity, always fully recovering from the previous step, with a small constant drift towards higher resistances. In conclusion, it can be said that the repeatability and stability were verified, enabling these polymeric gas sensors for different practical applications.

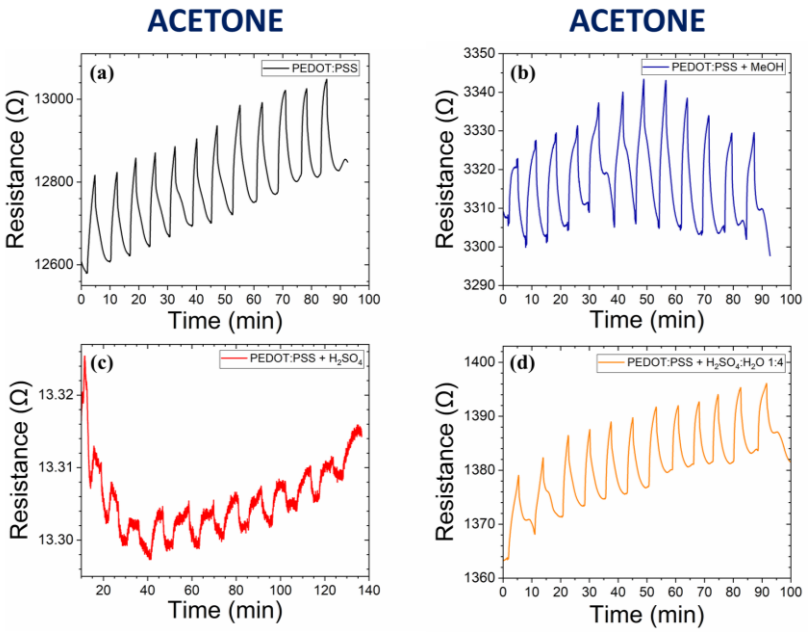

Figure 11: 12 cycles real-time measurements towards acetone at a fixed concentration of 5% of saturated vapor at room temperature for (a) pristine PEDOT:PSS, (b) PEDOT:PSS doped with MeOH, (c) PEDOT:PSS doped with concentrated H_2SO_4 and (d) PEDOT:PSS doped with 1:4 dilution of H_2SO_4.

As a final step, the effect of temperature was studied over a range from 10 °C up to 60 °C. From Figure 12, it is interesting to observe that increasing the temperature, the sensors performance decreased, except for the films doped with H_2SO_4 that also presented the lowest response. The best performances were obtained at 10 °C. After a sharp reduction, raising the temperature from 30 °C to 60°C, the gas response was almost unaltered.

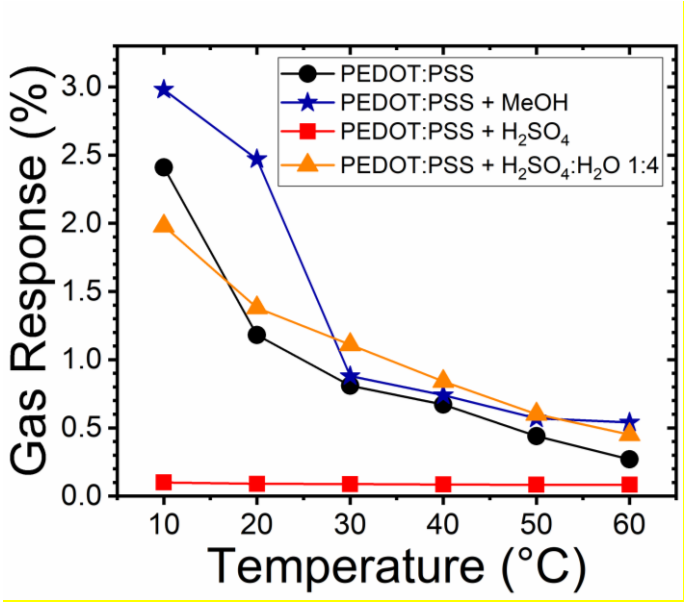

Figure 12: Gas sensing response of pristine PEDOT:PSS, PEDOT:PSS MeOH doped and PEDOT:PSS H_2SO_4 doped sensors as a function of the temperature towards 5% of saturated vapor of acetone.

Concerning the sensing mechanism, different theories have been proposed for the conducting polymer systems including redox reactions between the polymer chains and the analytes, charge transfer and polymer swelling [3,50,56,68]. It's difficult to have a clear understanding of the mechanism

490 governing the interaction of PEDOT:PSS with the analyte because, most of the time, it's a
491 combination of all of them where one is slightly predominant with respect to the others. The sensing
492 response is affected by the polymer oxidation level which is influenced by primary and secondary
493 doping. In PEDOT:PSS electrons in π-bonds are delocalized along the polymer chain due to the π-
494 orbital overlapping and they are responsible for the carrier's transportation. The effects of doping
495 undertake changes that contribute to make PEDOT:PSS encompassing near metallic to
496 semiconductor or insulating behavior. More in detail, the sensing mechanism taking place through
497 conduction occurs by intra- and inter-chain transport that can be affected by multiple factors. Through
498 secondary doping post treatments, defect density, chain orientation and crystallinity can be tuned.
499 Hence, PEDOT:PSS assumes an extended conjugation favoring a more regioregularity of the polymer
500 tertiary structure. In this way, there are more active sites for the interaction between gas molecules
501 and the conductive polymer. Furthermore, the reduction of PEDOT:PSS thickness upon secondary
502 doping implies an enhancement of volumetric capacitance and, consequently, its attitude at
503 implementing an efficient electrochemical activity in presence of oxidizing/reducing agents. By
504 immersing the electronic devices in the dopant baths, the further oxidation introduces polarons and
505 bipolarons as energy states between the LUMO and the HOMO [3,81]. Thus, it is important noting
506 that the removing of electrons leads not only to the appearance of oxidizing states but to a change of
507 the electronic structure, drastically reducing the 5.33 eV band gap in the neutral state [81]. It is also
508 noteworthy that the spatial extent of polaron and bipolaron states is smaller but still comparable to
509 the length of PEDOT polymer chains. For this reason, the overlap between polaron/bipolaron
510 wavefunctions belonging to the same chain is strong in comparison to those belonging to the
511 neighboring ones. Hence, the intra-chain hopping rate is estimated to greatly exceed the inter-chain
512 one due to the alignment of the crystallite, and therefore for the PEDOT:PSS, the inter-chain motion
513 represents the bottleneck determining the electron mobility and it is dictated by the tertiary structure
514 influenced by the packing arrangement. This kind of conduction is of essential importance because
515 most polymer chains do not extend between the gap across electrodes.
516 When the gas molecules interact with the surface of the sensing film, the hydrophilic PSS matrix,
517 upon which smaller PEDOT chains are bound, present a swelling process where adsorbates increase
518 the carriers hopping distance for charge transport creating an increase in electrical resistance for all
519 analytes. At the same time, interaction between the PEDOT chains and the vapors, due to redox
520 reactions, reversibly alter the conductivity and thus the presence of polarons and bipolarons on the
521 backbone of the polymer by transferring electrons/holes and delocalizing the conjugated π-electrons
522 of the sensing film. In fact, gas molecules behave as electrons donors/acceptors contributing a charge
523 carrier to the polymer and consequently participating as dopants that reversibly increase or decrease

the carrier concentration, respectively and the measured signal variation. In summary, the doping process is crucial in enhancing electrical conductivity that is strictly related to the sensing mechanism and thus the sensing performance.

4. CONCLUSIONS

This work illustrates a simple yet robust treatment method for the irreversible secondary doping of PEDOT:PSS in order to significantly enhance conductivity and improve gas sensing performance. For this reason, PEDOT:PSS gas sensors have been successfully fabricated by ink-jet printing technique and post-treated by immersing thin films in H_2SO_4 with different concentrations and pure MeOH. In both cases, the conductivity was enhanced due to the combined effects of chain linearization from a random coil structure, increased doping level through further oxidation and removal of insulating PSS chains leading to a better connection of the PEDOT domain. Contact angle measurements, thickness evaluation, FTIR spectroscopy and real time gas sensing tests were performed by exposing the devices with eight analytes with different chemical and physical properties. Furthermore, the MeOH-doped sensor displayed the best sensing response towards all VOCs investigated, except O_2 and NH_3. It was noticed that pure H_2SO_4 affects the gas response, decreasing the sensitivity due to a possible PEDOT:PSS over-doping and, surprisingly, inverting the behavior of a p-type semiconductor. The H_2SO_4:H_2O 2:1 solution still showed the same trend with an increased gas response, while further dilution caused a change in behavior in accordance with pristine PEDOT:PSS. The H_2SO_4:H_2O 1:4 solution exhibited the best responses, improving pristine PEDOT:PSS performance. As the dilution concentration increased, the sensing response improved with values comparable with the MeOH doped sensor. All of the thin films exhibited a higher response towards NO_2 with respect to VOCs vapors, allowing them to be utilized for a wide range of different applications. Further investigation could be performed in order to exploit the same material with a dual nature and improved selectivity by different secondary doping for the implementation of a simple and selective electronic nose prototype.

ACKNOWLEDGMENT

The Authors want to acknowledge for their help with the NO_x sensing measurements and set-up Andrea Marchisio and Jean Marc Tulliani.

REFERENCES

[1] H. Gerhard, J. Friedrich, Poly(alkylenedioxythiophene)s - new, very stable conducting polymers, Adv. Mater. 4 (1992) 116–118.

[2] F.D. Jonas, G.D. Heywang, W. Schmidtberg, J.P.D. Heinze, M. Dietrich, Polythiophenes,

process for their preparation and their use, EP339340, 1988.

[3] J.R. Reynolds, B.T. Thompson, T.A. Skotheim, Conjugated Polymers Properties, Processing, and Applications, 4th ed., CRC Press, 2019.

[4] T. Kim, S. Park, J. Seo, C.W. Lee, J.M. Kim, Highly conductive PEDOT:PSS with enhanced chemical stability, Org. Electron. 74 (2019) 77–81. https://doi.org/10.1016/j.orgel.2019.06.033.

[5] L. Groenendaal, F. Jonas, D. Freitag, H. Pielartzik, J.R. Reynolds, Poly(3,4-ethylenedioxythiophene) and its derivatives: past, present, and future, Adv. Mater. 12 (2000) 481–494. https://doi.org/10.1002/(SICI)1521-4095(200004)12:7<481::AID-ADMA481>3.0.CO;2-C.

[6] J. Ouyang, C.W. Chu, F.C. Chen, Q. Xu, Y. Yang, High-conductivity poly(3,4-ethylenedioxythiophene):poly(styrene sulfonate) film and its application in polymer optoelectronic devices, Adv. Funct. Mater. 15 (2005) 203–208. https://doi.org/10.1002/adfm.200400016.

[7] K. Yasumoro, Y. Fujita, H. Arimatsu, T. Fujima, A new composite structure of PEDOT/PSS: Macro-separated layers by a polyelectrolyte brush, Polymers (Basel). 12 (2020). https://doi.org/10.3390/polym12020456.

[8] C. Qiu, J. Wang, S. Mao, W. Guo, S. Cheng, Y. Wang, 2009 - Wang - Preparation of PEDOT PSS composite and its applications in anti-static coating, Polym. Adv. Technol. 21 (2010) 651–655.

[9] S. Zhang, E. Hubis, G. Tomasello, G. Soliveri, P. Kumar, F. Cicoira, Patterning of Stretchable Organic Electrochemical Transistors, Chem. Mater. 29 (2017) 3126–3132. https://doi.org/10.1021/acs.chemmater.7b00181.

[10] V. Bertana, G. Scordo, M. Parmeggiani, L. Scaltrito, S. Ferrero, M.G. Gomez, M. Cocuzza, D. Vurro, P. D'Angelo, S. Iannotta, C.F. Pirri, S.L. Marasso, Rapid prototyping of 3D Organic Electrochemical Transistors by composite photocurable resin, Sci. Rep. 10 (2020) 1–11. https://doi.org/10.1038/s41598-020-70365-8.

[11] S.M. Kim, C.H. Kim, Y. Kim, N. Kim, W.J. Lee, E.H. Lee, D. Kim, S. Park, K. Lee, J. Rivnay, M.H. Yoon, Influence of PEDOT:PSS crystallinity and composition on electrochemical transistor performance and long-term stability, Nat. Commun. 9 (2018). https://doi.org/10.1038/s41467-018-06084-6.

[12] A. Narayana, S.U. Kumar, N. Tarannum, S. V. Lokesh, High Performance Room Temperature Ethanol Detection Using Organic Field Effect Transistors Based on Polymer and Low Cost SnO_2 Nanoparticles Synthesized from Aegle Marmelos Fruit , Sens. Lett. 17 (2019) 581–586. https://doi.org/10.1166/sl.2019.4113.

[13] V. Preziosi, M. Barra, A. Perazzo, G. Tarabella, R. Agostino, S.L. Marasso, P. D'Angelo, S. Iannotta, A. Cassinese, S. Guido, Monitoring emulsion microstructure by Organic Electrochemical Transistors, J. Mater. Chem. C. 5 (2017) 2056–206. https://doi.org/10.1039/C6TC05149A.

[14] P. D'Angelo, S.L. Marasso, A. Verna, A. Ballesio, M. Parmeggiani, A. Sanginario, G. Tarabella, D. Demarchi, C.F. Pirri, M. Cocuzza, S. Iannotta, Scaling Organic

Electrochemical Transistors Down to Nanosized Channels, Small. 1902332 (2019) 1902332. https://doi.org/10.1002/smll.201902332.

[15] S. Anastasova, B. Crewther, P. Bembnowicz, V. Curto, H.M. Ip, B. Rosa, G.Z. Yang, A wearable multisensing patch for continuous sweat monitoring, Biosens. Bioelectron. 93 (2017) 139–145. https://doi.org/10.1016/j.bios.2016.09.038.

[16] S. Li, S. Chen, B. Zhuo, Q. Li, W. Liu, X. Guo, Flexible ammonia sensor based on PEDOT:PSS/silver nanowire composite film for meat freshness monitoring, IEEE Electron Device Lett. 38 (2017) 975–978. https://doi.org/10.1109/LED.2017.2701879.

[17] T. Wu, E. Gray, B. Chen, A self-healing, adaptive and conductive polymer composite ink for 3D printing of gas sensors, J. Mater. Chem. C. 6 (2018) 6200–6207. https://doi.org/10.1039/c8tc01092g.

[18] L. V. Kayser, D.J. Lipomi, Stretchable Conductive Polymers and Composites Based on PEDOT and PEDOT:PSS, Adv. Mater. 31 (2019). https://doi.org/10.1002/adma.201806133.

[19] S. Battistoni, C. Peruzzi, A. Verna, S.L. Marasso, M. Cocuzza, V. Erokhin, S. Iannotta, Synaptic response in organic electrochemical transistor gated by a graphene electrode, Flex. Print. Electron. 4 (2019) 044002. https://doi.org/10.1088/2058-8585/ab4dce.

[20] G. Tarabella, S.L. Marasso, V. Bertana, D. Vurro, P. D'Angelo, S. Iannotta, M. Cocuzza, Multifunctional Operation of an Organic Device with Three-Dimensional Architecture, Materials (Basel). 12 (2019) 1357. https://doi.org/10.3390/ma12081357.

[21] G. Scordo, V. Bertana, L. Scaltrito, S. Ferrero, M. Cocuzza, S.L. Marasso, S. Romano, R. Sesana, F. Catania, C.F. Pirri, A novel highly electrically conductive composite resin for stereolithography, Mater. Today Commun. 19 (2019) 12–17. https://doi.org/10.1016/j.mtcomm.2018.12.017.

[22] V. Bertana, G. Scordo, M. Manachino, S. Romano, M.G. Gomez, S.L. Marasso, S. Ferrero, M. Cocuzza, C.F. Pirri, L. Scaltrito, 3D Printed Active Objects based on the Promising PEDOT: PSS Resin: Investigation of their Integration inside an Electronic Circuit, Int. J. Eng. Res. Technol. 13 (2020) 462. https://doi.org/10.37624/IJERT/13.3.2020.462-469.

[23] G. Massaglia, A. Chiodoni, S.L. Marasso, C.F. Pirri, M. Quaglio, Electrical Conductivity Modulation of Crosslinked Composite Nanofibers Based on PEO and PEDOT:PSS, J. Nanomater. 2018 (2018) 1–7. https://doi.org/10.1155/2018/3286901.

[24] J. Jang, M. Chang, H. Yoon, Chemical sensors based on highly conductive poly(3,4-ethylene- dioxythiophene) nanorods, Adv. Mater. 17 (2005) 1616–1620. https://doi.org/10.1002/adma.200401909.

[25] A. Hasani, H. Sharifi Dehsari, M. Asghari Lafmejani, A. Salehi, F. Afshar Taromi, K. Asadi, S.Y. Kim, Ammonia-Sensing Using a Composite of Graphene Oxide and Conducting Polymer, Phys. Status Solidi - Rapid Res. Lett. 12 (2018) 1–7. https://doi.org/10.1002/pssr.201800037.

[26] D. Lv, W. Chen, W. Shen, M. Peng, X. Zhang, R. Wang, L. Xu, W. Xu, W. Song, R. Tan, Enhanced flexible room temperature ammonia sensor based on PEDOT: PSS thin film with $FeCl_3$ additives prepared by inkjet printing, Sensors Actuators B Chem. 298 (2019) 126890. https://doi.org/10.1016/j.snb.2019.126890.

[27] S. Shinde, C.Y. Jiang, C.X. Zheng, Y.Z. Wang, K.M. Lin, P.M. Koinkar, Room-temperature and flexible PEDOT:PSS-WO_3 gas sensor for nitrogen dioxide detection, in: Mod. Phys. Lett. B, World Scientific Publishing Co. Pte Ltd, 2019. https://doi.org/10.1142/S021798491940013X.

[28] I. Marr, T. Stöcker, R. Moos, F3 - Resistives Gasdosimeter auf Basis von PEDOT:PSS zur Detektion von NO und NO_2, in: 11. Dresdner Sensor-Symposium, 2013: pp. 317–320. https://doi.org/10.5162/11dss2013/f3.

[29] C.J. Chiang, K.T. Tsai, Y.H. Lee, H.W. Lin, Y.L. Yang, C.C. Shih, C.Y. Lin, H.A. Jeng, Y.H. Weng, Y.Y. Cheng, K.C. Ho, C.A. Dai, In situ fabrication of conducting polymer composite film as a chemical resistive CO_2 gas sensor, Microelectron. Eng. 111 (2013) 409–415. https://doi.org/10.1016/j.mee.2013.04.014.

[30] S. Rattan, P. Singhal, A.L. Verma, Synthesis of PEDOT:PSS (poly(3,4-ethylenedioxythiophene))/poly(4-styrene sulfonate))/ ngps (nanographitic platelets) nanocomposites as chemiresistive sensors for detection of nitroaromatics, Polym. Eng. Sci. 53 (2013) 2045–2052. https://doi.org/10.1002/pen.23466.

[31] H. Yoon, Current Trends in Sensors Based on Conducting Polymer Nanomaterials, Nanomaterials. 3 (2013) 524–549. https://doi.org/10.3390/nano3030524.

[32] Y. Seekaew, S. Lokavee, D. Phokharatkul, A. Wisitsoraat, T. Kerdcharoen, C. Wongchoosuk, Low-cost and flexible printed graphene-PEDOT:PSS gas sensor for ammonia detection, Org. Electron. 15 (2014) 2971–2981. https://doi.org/10.1016/j.orgel.2014.08.044.

[33] S. Sharma, S. Hussain, S. Singh, S.S. Islam, MWCNT-conducting polymer composite based ammonia gas sensors: A new approach for complete recovery process, Sensors Actuators, B Chem. 194 (2014) 213–219. https://doi.org/10.1016/j.snb.2013.12.050.

[34] Y. Zheng, D. Lee, H.Y. Koo, S. Maeng, Chemically modified graphene/PEDOT:PSS nanocomposite films for hydrogen gas sensing, Carbon N. Y. 81 (2015) 54–62. https://doi.org/10.1016/j.carbon.2014.09.023.

[35] S. Pecqueur, S. Lenfant, D. Guérin, F. Alibart, D. Vuillaume, Concentric-electrode organic electrochemical transistors: Case study for selective hydrazine sensing, Sensors (Switzerland). 17 (2017). https://doi.org/10.3390/s17030570.

[36] N. Tang, Y. Jiang, H. Qu, X. Duan, Conductive polymer nanowire gas sensor fabricated by nanoscale soft lithography, Nanotechnology. 28 (2017). https://doi.org/10.1088/1361-6528/aa905b.

[37] C.M. Hangarter, S.C. Hernandez, X. He, N. Chartuprayoon, Y.H. Choa, N. V. Myung, Tuning the gas sensing performance of single PEDOT nanowire devices, Analyst. 136 (2011) 2350–2358. https://doi.org/10.1039/c0an01000f.

[38] J. Choi, D.W. Park, S.E. Shim, Electrospun PEDOT:PSS/carbon nanotubes/PVP nanofibers as chemiresistors for aromatic volatile organic compounds, Synth. Met. 162 (2012) 1513–1518. https://doi.org/10.1016/j.synthmet.2012.06.028.

[39] S. Badhulika, N. V. Myung, A. Mulchandani, Conducting polymer coated single-walled carbon nanotube gas sensors for the detection of volatile organic compounds, Talanta. 123 (2014) 109–114. https://doi.org/10.1016/j.talanta.2014.02.005.

[40] A. Hasani, H.S. Dehsari, J.N. Gavgani, E.K. Shalamzari, A. Salehi, F. Afshar Taromi, M. Mahyari, Sensor for volatile organic compounds using an interdigitated gold electrode modified with a nanocomposite made from poly(3,4-ethylenedioxythiophene)-poly(styrenesulfonate) and ultra-large graphene oxide, Microchim. Acta. 182 (2015) 1551–1559. https://doi.org/10.1007/s00604-015-1487-7.

[41] A. Kaushik, R. Kumar, S.K. Arya, M. Nair, B.D. Malhotra, S. Bhansali, Organic-Inorganic Hybrid Nanocomposite-Based Gas Sensors for Environmental Monitoring, Chem. Rev. 115 (2015) 4571–4606. https://doi.org/10.1021/cr400659h.

[42] J. Dai, O. Ogbeide, N. Macadam, Q. Sun, W. Yu, Y. Li, B.L. Su, T. Hasan, X. Huang, W. Huang, Printed gas sensors, Chem. Soc. Rev. 49 (2020) 1756–1789. https://doi.org/10.1039/c9cs00459a.

[43] A. Schütze, T. Baur, M. Leidinger, W. Reimringer, R. Jung, T. Conrad, T. Sauerwald, Highly sensitive and selective VOC sensor systems based on semiconductor gas sensors: How to?, Environ. - MDPI. 4 (2017) 1–13. https://doi.org/10.3390/environments4010020.

[44] T. Boningari, P.G. Smirniotis, Impact of nitrogen oxides on the environment and human health: Mn-based materials for the NO_x abatement, Curr. Opin. Chem. Eng. 13 (2016) 133–141. https://doi.org/10.1016/j.coche.2016.09.004.

[45] L.N. Lamsal, R. V. Martin, A. Padmanabhan, A. Van Donkelaar, Q. Zhang, C.E. Sioris, K. Chance, T.P. Kurosu, M.J. Newchurch, Application of satellite observations for timely updates to global anthropogenic NO_x emission inventories, Geophys. Res. Lett. 38 (2011) 1–5. https://doi.org/10.1029/2010GL046476.

[46] M. Kampa, E. Castanas, Human health effects of air pollution, Environ. Pollut. 151 (2008) 362–367. https://doi.org/10.1016/j.envpol.2007.06.012.

[47] Department Of Health And Human Services Centers for Disease Control and Prevention National Institute for Occupational Safety and Health, NIOSH Pocket Guide To Chemical Hazards, 2007. https://doi.org/10.1109/icnn.1993.298588.

[48] Y. Wang, A. Liu, Y. Han, T. Li, Sensors based on conductive polymers and their composites: a review, Polym. Int. 69 (2020) 7–17. https://doi.org/10.1002/pi.5907.

[49] A.G. MacDiarmid, A.J. Epstein, The concept of secondary doping as applied to polyaniline, Synth. Met. 65 (1994) 103–116. https://doi.org/10.1016/0379-6779(94)90171-6.

[50] Y.C. Wong, B.C. Ang, A.S.M.A. Haseeb, A.A. Baharuddin, Y.H. Wong, Review—Conducting Polymers as Chemiresistive Gas Sensing Materials: A Review, J. Electrochem. Soc. 167 (2020) 037503. https://doi.org/10.1149/2.0032003jes.

[51] D. Alemu, H.Y. Wei, K.C. Ho, C.W. Chu, Highly conductive PEDOT:PSS electrode by simple film treatment with methanol for ITO-free polymer solar cells, Energy Environ. Sci. 5 (2012) 9662–9671. https://doi.org/10.1039/c2ee22595f.

[52] A.J. Oostra, K.H.W. Van Den Bos, P.W.M. Blom, J.J. Michels, Disruption of the electrical conductivity of highly conductive poly(3,4-ethylenedioxythiophene):poly(styrene sulfonate) by hypochlorite, J. Phys. Chem. B. 117 (2013) 10929–10935. https://doi.org/10.1021/jp4050836.

[53] W. Meng, R. Ge, Z. Li, J. Tong, T. Liu, Q. Zhao, S. Xiong, F. Jiang, L. Mao, Y. Zhou, Conductivity Enhancement of PEDOT:PSS Films via Phosphoric Acid Treatment for Flexible All-Plastic Solar Cells, ACS Appl. Mater. Interfaces. 7 (2015) 14089–14094. https://doi.org/10.1021/acsami.5b03309.

[54] C.S. Pathak, J.P. Singh, R. Singh, Optimizing the electrical properties of PEDOT:PSS films by co-solvents and their application in polymer photovoltaic cells, Appl. Phys. Lett. 111 (2017). https://doi.org/10.1063/1.4994317.

[55] F. Wu, P. Li, K. Sun, Y. Zhou, W. Chen, J. Fu, M. Li, S. Lu, D. Wei, X. Tang, Z. Zang, L. Sun, X. Liu, J. Ouyang, Conductivity Enhancement of PEDOT:PSS via Addition of Chloroplatinic Acid and Its Mechanism, Adv. Electron. Mater. 3 (2017). https://doi.org/10.1002/aelm.201700047.

[56] C.M. Hangarter, N. Chartuprayoon, S.C. Hernández, Y. Choa, N. V. Myung, Hybridized conducting polymer chemiresistive nano-sensors, Nano Today. 8 (2013) 39–55. https://doi.org/10.1016/j.nantod.2012.12.005.

[57] A.G. MacDiarmid, A.J. Epstein, Secondary doping in polyaniline, Synth. Met. 69 (1995) 85–92. https://doi.org/10.1016/s0379-6779(96)03842-8.

[58] J.Y. Kim, J.H. Jung, D.E. Lee, J. Joo, Enhancement of electrical conductivity of poly(3, 4-ethylenedioxythiophene)/poly(4-styrenesulfonate) by a change of solvents, Synth. Met. 126 (2002) 311–316. https://doi.org/10.1016/S0379-6779(01)00576-8.

[59] H. Shi, C. Liu, Q. Jiang, J. Xu, Effective Approaches to Improve the Electrical Conductivity of PEDOT:PSS: A Review, Adv. Electron. Mater. 1 (2015). https://doi.org/10.1002/aelm.201500017.

[60] L. Salucci, Process optimization and experimental measurements of organic electrochemical transistors for in liquid biosensing, Politencico di Torino, 2019.

[61] L. Vigna, A. Fasoli, M. Cocuzza, F.C. Pirri, L.D. Bozano, M. Sangermano, A Flexible, Highly Sensitive, and Selective Chemiresistive Gas Sensor Obtained by In Situ Photopolymerization of an Acrylic Resin in the Presence of MWCNTs, Macromol. Mater. Eng. 1800453 (2018) 1800453. https://doi.org/10.1002/mame.201800453.

[62] J.A. Dean, Lange'S Handbook of Chemistry, 15th ed., McGraw-Hill, New York, 1999. https://doi.org/10.1080/10426919008953291.

[63] E. Araujo-Lopez, J.S. Lopez-Echeverry, S. Reif-Acherman, The Antoine equation of state: Rediscovering the potential of an almost forgotten expression for calculating volumetric properties of pure compounds, Chem. Eng. Sci. 177 (2018) 89–109. https://doi.org/10.1016/j.ces.2017.10.051.

[64] P. Kar, N.C. Pradhan, B. Adhikari, Application of sulfuric acid doped poly (m-aminophenol) as aliphatic alcohol vapor sensor material, Sensors Actuators, B Chem. 140 (2009) 525–531. https://doi.org/10.1016/j.snb.2009.05.013.

[65] D. Green, M.Z. Southard, Perry's Chemical Engineers Handbook, 7th Ed, McGraw-Hill Education, 1997.

[66] S.K.M. Jönsson, J. Birgerson, X. Crispin, G. Greczynski, W. Osikowicz, A.W. Denier van

762 der Gon, W.R. Salaneck, M. Fahlman, The effects of solvents on the morphology and sheet
763 resistance in poly(3,4-ethylenedioxythiophene)-polystyrenesulfonic acid (PEDOT-PSS)
764 films, Synth. Met. 139 (2003) 1–10. https://doi.org/10.1016/S0379-6779(02)01259-6.

765 [67] T.H. Meen, K.L. Chen, Y.H. Chen, W.R. Chen, D.W. Chou, W.H. Lan, C.J. Huang, The
766 effects of dilute sulfuric acid on sheet resistance and transmittance in poly(3,4-
767 thylenedioxythiophene): Poly(styrenesulfonate) films, Int. J. Photoenergy. 2013 (2013).
768 https://doi.org/10.1155/2013/843410.

769 [68] Hosseini, The Key Mechanism of Conductivity in PEDOT-PSS Thin Films Exposed by
770 Anomalous Conduction Behaviour upon Solvent-Doping and Sulfuric Acid Post
771 Treatment.pdf, J. Mater. Chem. C. (2020).

772 [69] S.S. Yoon, D.Y. Khang, Roles of Nonionic Surfactant Additives in PEDOT:PSS Thin Films,
773 J. Phys. Chem. C. 120 (2016) 29525–29532. https://doi.org/10.1021/acs.jpcc.6b12043.

774 [70] Y. Xia, K. Sun, J. Ouyang, Solution-processed metallic conducting polymer films as
775 transparent electrode of optoelectronic devices, Adv. Mater. 24 (2012) 2436–2440.
776 https://doi.org/10.1002/adma.201104795.

777 [71] Z. Zhu, C. Liu, F. Jiang, J. Xu, E. Liu, Effective treatment methods on PEDOT:PSS to
778 enhance its thermoelectric performance, Synth. Met. 225 (2017) 31–40.
779 https://doi.org/10.1016/j.synthmet.2016.11.011.

780 [72] S.R.S. Kumar, N. Kurra, H.N. Alshareef, Enhanced high temperature thermoelectric response
781 of sulphuric acid treated conducting polymer thin films, J. Mater. Chem. C. 4 (2015) 215–
782 221. https://doi.org/10.1039/c5tc03145a.

783 [73] C.M. Palumbiny, C. Heller, C.J. Schaffer, V. Körstgens, G. Santoro, S. V. Roth, P. Müller-
784 Buschbaum, Molecular reorientation and structural changes in cosolvent-treated highly
785 conductive PEDOT:PSS electrodes for flexible indium tin oxide-free organic electronics, J.
786 Phys. Chem. C. 118 (2014) 13598–13606. https://doi.org/10.1021/jp501540y.

787 [74] A.M. Nardes, R.A.J. Janssen, M. Kemerink, A morphological model for the solvent-
788 enhanced conductivity of PEDOT:PSS thin films, Adv. Funct. Mater. 18 (2008) 865–871.
789 https://doi.org/10.1002/adfm.200700796.

790 [75] N.B. Colthup, L.H. Daly, S.E. Wiberley, Introduction to infrared and Raman spectroscopy,
791 Academic P, Waltham, 1990. https://doi.org/doi:10.1016.

792 [76] K. Nakamoto, Infrared and Raman Spectra of Inorganic and Coordination Compounds: Part
793 B: Applications in Coordination, Organometallic, and Bioinorganic Chemistry, John Wiley
794 & Sons, New York, 1997. https://doi.org/10.1002/9780470405888.

795 [77] G.M. Neelgund, E. Hrehorova, M. Joyce, V. Bliznyuk, Synthesis and characterization of
796 polyaniline derivative and silver nanoparticle composites, Polym Int. 55 (2006) 961–969.
797 https://doi.org/DOI: 10.1002/pi.2445.

798 [78] N. Kim, S. Kee, S.H. Lee, B.H. Lee, Y.H. Kahng, Y.R. Jo, B.J. Kim, K. Lee, Highly
799 conductive PEDOT:PSS nanofibrils induced by solution-processed crystallization, Adv.
800 Mater. 26 (2014) 2268–2272. https://doi.org/10.1002/adma.201304611.

801 [79] A. Zykwinska, W. Domagala, B. Pilawa, M. Lapkowski, Electrochemical overoxidation of

poly(3,4-ethylenedioxythiophene) - PEDOT studied by means of in situ ESR spectroelectrochemistry, in: Electrochim. Acta, 2005: pp. 1625–1633. https://doi.org/10.1016/j.electacta.2004.10.026.

[80] P. Tehrani, A. Kanciurzewska, X. Crispin, N.D. Robinson, M. Fahlman, M. Berggren, The effect of pH on the electrochemical over-oxidation in PEDOT:PSS films, Solid State Ionics. 177 (2007) 3521–3527. https://doi.org/10.1016/j.ssi.2006.10.008.

[81] I. Zozoulenko, A. Singh, S.K. Singh, V. Gueskine, X. Crispin, M. Berggren, Polarons, Bipolarons, And Absorption Spectroscopy of PEDOT, ACS Appl. Polym. Mater. 1 (2019) 83–94. https://doi.org/10.1021/acsapm.8b00061.